Available online at www.sciencedirect.com

ScienceDirect

Procedia IUTAM 11 (2014) 23 – 33

Procedia IUTAM

www.elsevier.com/locate/procedia

Nonlinear Interfacial Wave Phenomena from the Micro- to the Macro-Scale

Microfluidics in microstructure optical fibers: heat flux and pressure-driven and other flows

Paul Christodoulides[a,*], Georgios Florides[a], Kyriacos Kalli[a,b], Charalambos Koutsides[b], Lazaros Lazari[a], Michael Komodromos[c], Frédéric Dias[d,e]

[a]*Faculty of Engineering and Technology, Cyprus University of Technology, Limassol, Cyprus*
[b]*Nanophotonics Research Laboratory, Department of Electrical Engineering / Computer Engineering and Informatics, Cyprus University of Technology, Limassol, Cyprus*
[c]*Frederick University, Nicosia, Cyprus*
[d]*School of Mathematical Sciences, University College Dublin, Dublin, Ireland*
[e]*Centre de Mathématiques et de Leurs Applications, Ecole Normale Supérieure de Cachan and CNRS, Cachan, France*

Abstract

Microfluidics are important micro-scale devices that can be used to manipulate very small volumes of fluids on the order of nano- to femto-liters. The control and sorting of nano-particles is a primary goal using this technology. There is particular interest in the use of microstructure optical fibers for the heat transfer of fluids, whereby the guided light interacts with a fluid in the region of the air-hole structure.

We study the fluid transport capabilities of microstructure fibers with cross sections containing circular or elliptical holes, considering the effects of flow rates, fluid viscosity, and the channel shape. The role of heat flux is considered in relation to the fluid characteristics. Results can be obtained through the solution of the time-dependent Navier-Stokes equations and the convection-diffusion equation. This work is of importance as one cannot assume that the flow dynamics in microstructure fibers will be the same as conventional micro-fluidic channels. Through the study of the heat transfer, for pressure-driven and other flows and for low Reynolds numbers, we confirm anticipated behavior of the fluids in the micro-channel structure.

Keyword: Microfluidics, microstructure optical fiber, fluid flow, heat flux

doi:10.1016/j.piutam.2014.01.045

1. Introduction

Microfluidics is an important research field that relies on the use of micro-scale devices for the manipulation of very small volumes of fluids; typically on nano- to femto-litres. An attractive feature of this technology is the control and sorting of nano-particles, with the analysis of DNA in fluid streams proving of great interest for high throughput chemical and biological analysis. The need for small fluid channels is compatible with certain types of microstructure optical fibers. These fibers have a central waveguide surrounded by a series of air holes that run parallel to the optical axis and ensure low loss light propagation. In this case the guided light can interact with a fluid in the region of the air-hole structure[1,2,3]. Microstructure fibers have shown great potential as microfluidic devices, given the minute sample volumes that are required. Their use as optofluidic sensors is compatible with applications in chemical and biological sensing. Given the development of new types of microstructure fibers with cross sections containing circular or elliptical holes, or more complex cross sectional geometries, it is important to be able to model the fluid transport capabilities of these fiber types. Moreover, complex cross sectional geometries can affect the transfer of heat into the fiber, creating local changes in the behavior of the fluid system. In this paper these aforementioned effects are studied using a numerical application of a system of partial differential equations consisting of the time-dependent Navier-Stokes equations and the convection-diffusion equation. We examine the effects of flow rates, fluid viscosity and the channel shape. The role of heat flux is considered in relation to the fluid characteristics, but also with regard to the material properties of the microstructure fiber.

It is necessary to consider the behavior of microstructure fibers as microfluidic channels, as their dimensions are typically on the same scale as transitional micro channels; this is typically a factor of 10 smaller than conventional micro-fluidic channels. The features of a flow and any potential heat transfer are governed by the length scales and material properties, which in turn are governed by the Reynolds number and the convection heat transfer coefficient.

Although there have been many studies on micro-fluidic flows, one can mention as an indicative case related to the present study, Yanhg and collaborators' investigation of the fluid dynamics of microfluidic devices with multiple channels having trapezoidal and triangular cross sections[4]. Moreover Colin and Tancogne studied the stability of jets in micro-channels and computed the length on which a jet is stable for a given configuration with respect to the flow rates, viscosities, diameter of the channel and surface tension[5], whereas Sahu and collaborators studied the stability of a co-flow composed of a Newtonian and non-Newtonian fluid[6]. Lien and Vollmer detected minimum flow rates based on integrated optical fiber cantilevers[7]. Regarding heat transfer related to microfluidics the literature is not so extensive and includes the work of Beskok and Karniadakis, Chen and Wu, Damean and collaborators and Plouffe and collaborators[8.9,10,11].

In section 2 the mathematical model for the flow along a microchannel is formulated in conjunction with heat transfer. Numerical results for certain flow and heat configurations based on the Finite Element Method (FEM).are presented in section 3. Finally section 4 is devoted to a discussion for further numerical and experimental applications.

2. Flow along a microchannel

The general form of the Navier-Stokes equations (*momentum* equation) governing a three-dimensional motion of an *incompressible* fluid is given by (in summation-convention notation)

$$\rho \frac{\partial u_i}{\partial t} + \rho u_j \frac{\partial u_i}{\partial x_j} = f_i, \tag{1}$$

where ρ is the density of the fluid (in kg m^{-3}), u_i the velocity component of the fluid in the i-direction (in m s^{-1}) and f_i the total force per volume (in kg m^{-2} s^{-1}) acting on the fluid consisting of pressure gradient, friction forces and body forces. The continuity equation is given by

$$\frac{\partial u_i}{\partial x_i} = 0 \tag{2}$$

For small Knudsen numbers and in the absence of body forces and following the microfluidics simplifications (according to which gravity may be neglected and as the influence of convection is small, there is no convecting momentum transport) the governing equations may be written as follows.

$$\rho \frac{\partial u_i}{\partial t} = -\frac{\partial p}{\partial x_i} + \mu \frac{\partial^2 u_i}{\partial x_i^2} \tag{3}$$

with an extra equation for p, the fluid pressure (in Pa), arising by simply applying the divergence operator to the Navier-Stokes equation, and where μ is the dynamic viscosity of the fluid (in kg m^{-1} s^{-1}).

It is common place to re-write the system of equations above in dimensionless form (not done here for practical reasons). In such case the dimensionless Reynolds number is given by

$$\mathrm{Re} = \frac{\rho u_0 L}{\mu} \tag{4}$$

This describes the balance between inertial forces and viscosity, where u_0 is a fixed mean velocity relative to the fluid and L some fixed characteristic linear dimension. It is typical that viscous forces are dominant for flows in microchannels, corresponding to low Reynolds numbers. In general, microfluidic flows can be classified, according to their Reynolds number, as

(i) Creeping/Stokes (laminar) flows with no lateral convection (Re < 1),

(ii) *Intermediate* (still laminar) flows with lateral convection becoming increasingly important (1 < Re < 2300) (where time dependence becomes more important),

(iii) Turbulent flows, where there is a curling of field lines, perturbations are amplified and the development of field of velocity vectors over time is unpredictable (Re > 2300).

When interested in the energy transport into the material region, the energy equation in the fluid region is given by the convection-diffusion equation

$$\rho c_p \frac{\partial T}{\partial t} + \rho u_3 \frac{\partial T}{\partial x_3} + \frac{\partial}{\partial x_i}(-\lambda \frac{\partial T}{\partial x_i}) + h(T_{fluid} - T_{\mathrm{int}}) = 0. \tag{5}$$

Here h is the convection heat transfer coefficient (in W m^{-2} K^{-1}) multiplied by an appropriate coefficient depending on the cross-section configuration[12], λ the thermal fluid conductivity (in W m^{-1} K^{-1}), c_p the fluid specific heat capacity (in J kg^{-1} K^{-1}), and T_{fluid} and T_{int} are respectively the temperature of the fluid and the temperature at the wall of the channel. Coupling equation (4) to set of equations (2) will yield the full system describing the heat transfer in a flow domain. The particular model chosen here can indeed be considered as a first simplified case of a more complete mathematical model that could include the effects of electromagnetism (owing to the choice of the method of heating relating to the set-up of the microfluidics device) (see for example Plouffe and collaborators work on microfluidic magnetophoresis[11].

3. Numerical Results

The pressure-driven flow along a microchannel is considered, where a single circular or elliptical micro-capillary running along the length of the fiber axis is surrounded by a ring filled with gas. For appropriate boundary conditions, the coupled differential equations (3) and (5) are solved numerically, by application of the Finite Element Method (FEM). Considering the laminar character of the flow, we present here a constant velocity flow. The FlexPDE software package is chosen as the numerical solving tool that uses an Adaptive Mesh Refinement method. The FEM mesh is shown in Fig. 1 for both cases, along with a third configuration of a three-hole microstructure fiber, also surrounded by a gas-ring. The fiber length is taken to be 3 cm with a relatively thick diameter of d = 125 μm, while the ring has an internal diameter of 60 μm and an external one of 70 μm. For all cases presented here the fiber material is silica (SiO_2) and the gas in the ring is air (see Table 1 for thermal properties).

We first study the behavior of water (see Table 1 for its thermal properties) within a single circular channel of diameter of 15 μm (see Fig. 1a) with respect to external temperature, for a fixed fluid velocity of 0.05 m s^{-1} and an initial fluid temperature of 20°C.

Table 1. Physical properties.

Fluid or Fiber glass	ρ	μ	λ	c_p
	kg m^{-3}	kg m^{-1} s^{-1}	W m^{-1} K^{-1}	J kg^{-1} K^{-1}
Water	1000	0.001	0.609	4185
Olive oil	916	0.084	0.170	1970
Glycerine	1260	1.490	0.290	2430
Air	0.93	-	0.032	1010
SiO_2	2250	-	1.400	700

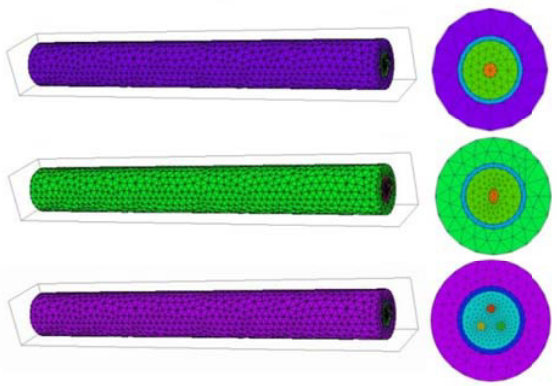

Fig. 1. FEM Mesh for a microstructure fiber with (top-to-bottom) (a) single-circular, capillary running along the length of the fiber axis and surrounded by a gas-ring, (b) single-elliptical capillary running along the length of the fiber axis and surrounded by a gas-ring (c) triple-circular micro-capillary.

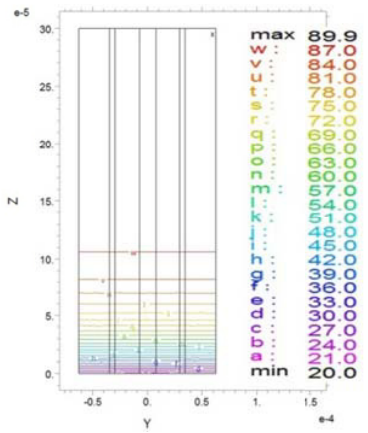

Fig. 2. Axial temperature distribution of the fiber with the circular microchannel for a flow of water with velocity of 0.005 m s^{-1} and temperature of 20oC and an external temperature of 90 oC (z is scaled for computational purposes).

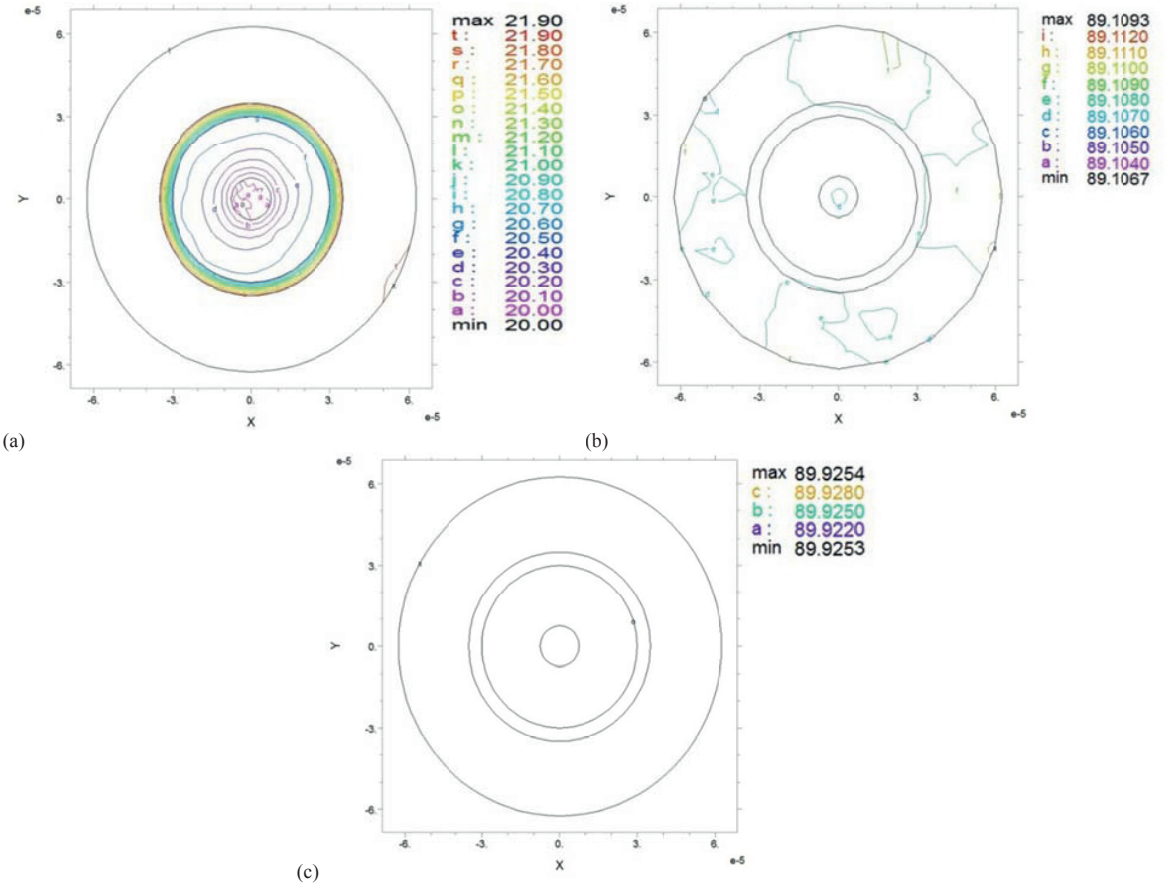

Fig. 3. Cross-sectional temperature distribution of the fiber with the circular microchannel for a flow of water with velocity of 0.005 m s^{-1} and temperature of 20°C and an external temperature of 90oC: (a) inlet temperature, (b) middle temperature, (c) outlet temperature.

An indicative flow case is presented in Figs. 2 and 3. In Fig. 2 the axial temperature distribution along the fiber is shown for an external temperature of 90oC. One can observe steady-state temperatures between 20 and 90oC within the channel. In Fig. 3 are shown three cross-sectional temperature distributions (inlet, middle and outlet).

The flow case presented above is repeated for a different external temperatures (in addition to 90°C) of 50°C. Fig. 4 shows the mid-channel temperature at its end with respect to time. In both cases the steady-state seems to be reached in about 40 s.

For the same optical fiber configuration (circular microchannel of diameter of 15 μm), we next study the effect of the fluid chosen (see Table 1 for their thermal properties) on the steady-state mid-channel temperature, for a fixed fluid velocity of 0.005 m s^{-1}, initial fluid temperature of 20°C and external temperature of 90°C. The results are shown in Fig. 5, where one can observe that in 50 s, water has the best cooling effect along the micro-channel, followed by glycerine and then oil.

We then turn our attention to the study of an elliptical microchannel of axes 15 μm and 10 μm (see Fig. 1b). An indicative flow case is presented in Figs. 6 and 7. In Fig. 6 the axial temperature distribution along the fiber channel at a time of 90 s is shown for an external temperature of 90 °C. for a water flow with velocity of 0.005 m s^{-1}. In Fig. 7 are shown three cross-sectional temperature distributions (inlet, middle and outlet).

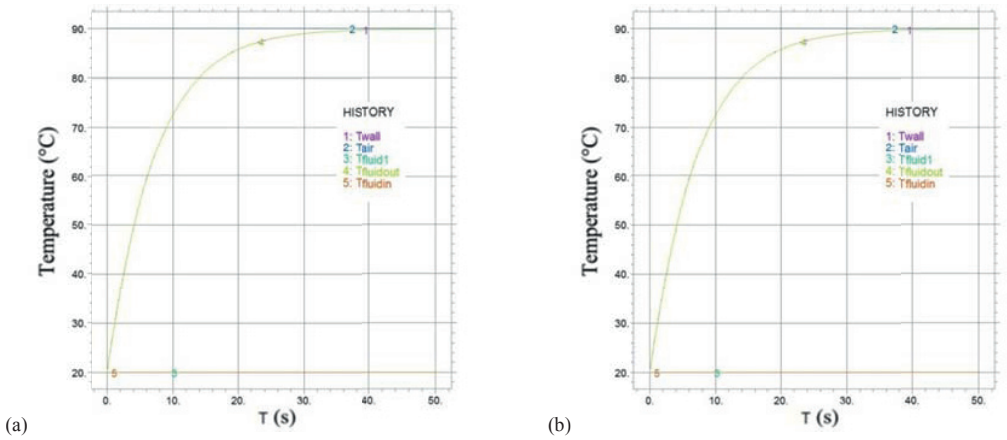

Fig. 4. Temperature with respect to time for water flow (in the circular microchannel) with velocity of 0.005 m s^{-1} and initial temperature of 20°C, for external temperatures of (a) 50°C, and (b) 90°C.

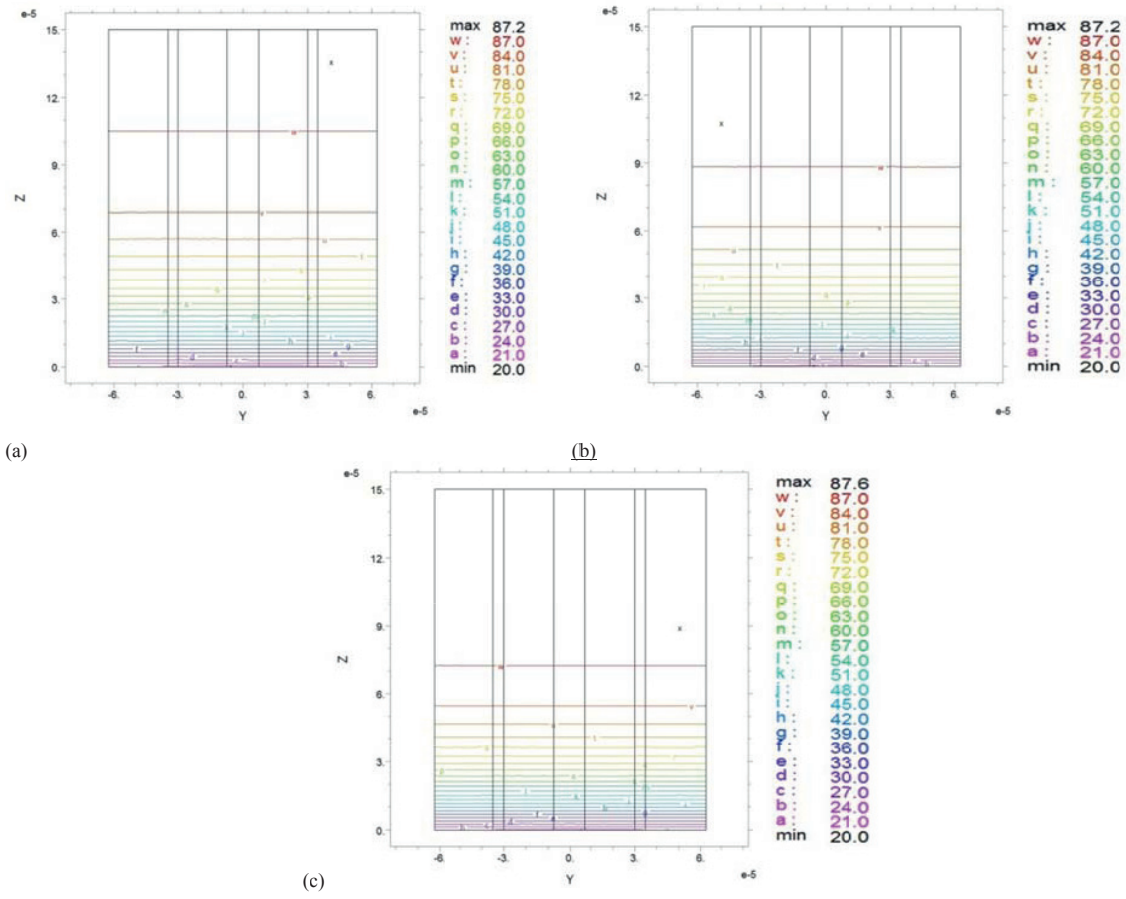

Fig. 5. Axial temperature distribution of the fiber with the circular microchannel for a fluid flow with velocity of 0.005 m s^{-1} and temperature of 20°C and an external temperature of 90 °C (*z* is scaled for computational purposes) when the fluid is (a) water, (b) glycerine and (c) oil.

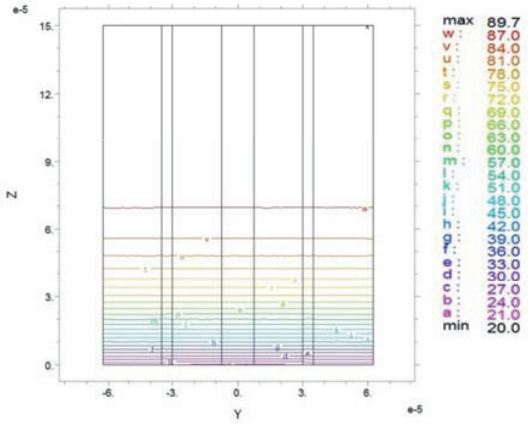

Fig. 6. Axial temperature distribution of the fiber with the elliptical microchannel at a time of 90 s for a flow of water with velocity of 0.005 m s^{-1} and temperature of 20ºC and an external temperature of 90 ºC (z is scaled for computational purposes).

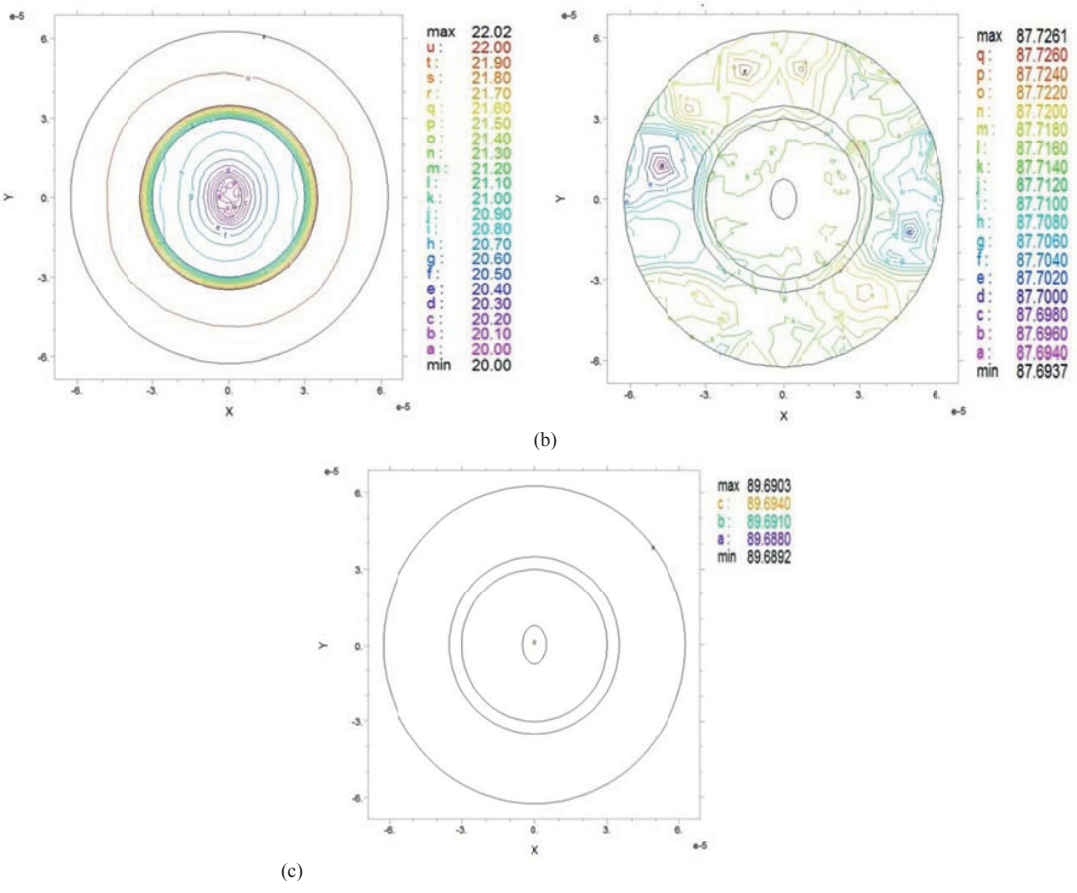

(a) (b)

(c)

Fig. 7. Cross-sectional temperature distribution of the fiber with the elliptical microchannel for a flow of water with velocity 0.005 m s^{-1} and temperature 20ºC and an external temperature of 90ºC: (a) inlet temperature, (b) middle temperature, (c) outlet temperature.

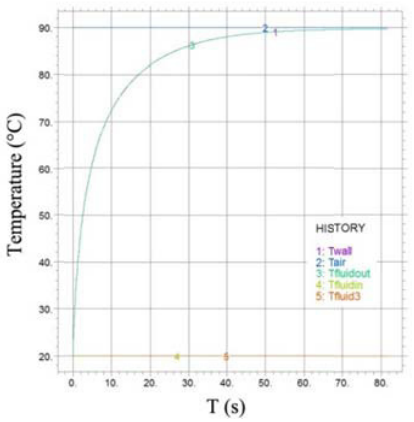

Fig. 8. Temperature with respect to time for water flow (in the elliptical microchannel) with velocity of 0.005 m s^{-1} and initial temperature of 20°C for an external temperature of 90°C.

For this particular case, the mid-channel temperature with respect to time is plotted in Fig. 8. The steady-state temperature is attained in 70 s as opposed to 40 s for the corresponding one for a circular channel presented in Fig. 4(b). It must be stressed that the decisive factor is not the shape of the channel but rather the size of the circumference. An elliptical microchannel of the same circumference (studied but not shown here) as the circular microchannel of Fig. 4 behaves in an identical manner with regard to its thermal properties.

In order to assess the behavior of a fluid within the microchannel with respect to velocity, we consider the mid-channel (at 1 cm from the inlet) steady-state temperature attained for different velocities. Fig. 9 shows that, for water, (as expected) the greater the velocity the lower the fluid temperature. The Reynolds numbers corresponding to these velocities are all low (Re << 1), and the flows can be considered as creeping laminar.

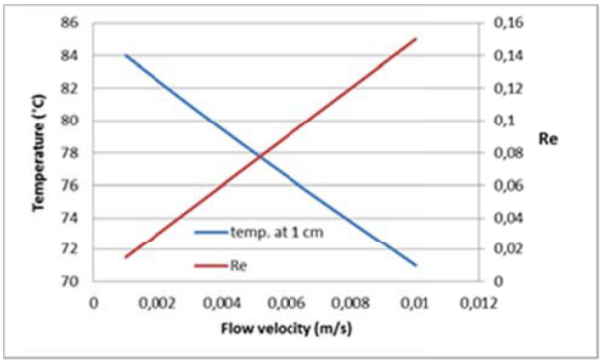

Fig. 9. For an external temperature of 90°C, the steady-state highest mid-channel temperature of water in the elliptical microchannel as a function of velocity for Reynolds number values of Re << 1. Clearly, the greater the velocity the lower the fluid temperature.

Finally, we study the triple-circular microchannel configuration (see Fig. 1c). The diameter of each circle is 8.66 μm with all circles' center being equidistant at 12 μm from the center of the fiber cross section. Again, an indicative flow case is presented in Figs. 10 and 11. In Fig. 10 the axial temperature distribution along the fiber is shown for an external temperature of 90°C. One can observe steady-state temperatures between 20 and 90°C within the channel. In Fig. 11 are shown three cross-sectional temperature distributions (inlet, middle and outlet).

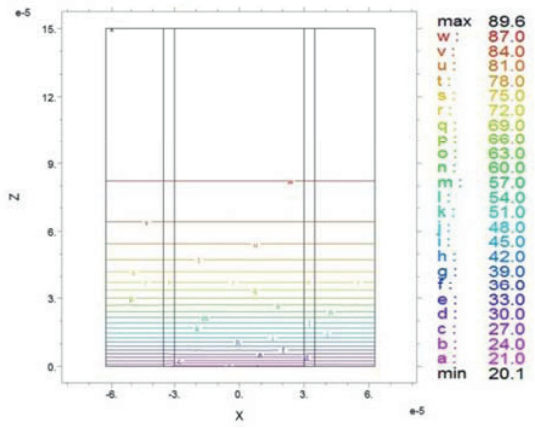

Fig. 10. Axial temperature distribution of the fiber with the triple-circular microchannels for a flow of water with velocity of 0.005 m s^{-1} and temperature of 20°C and an external temperature of 90 °C (z is scaled for computational purposes).

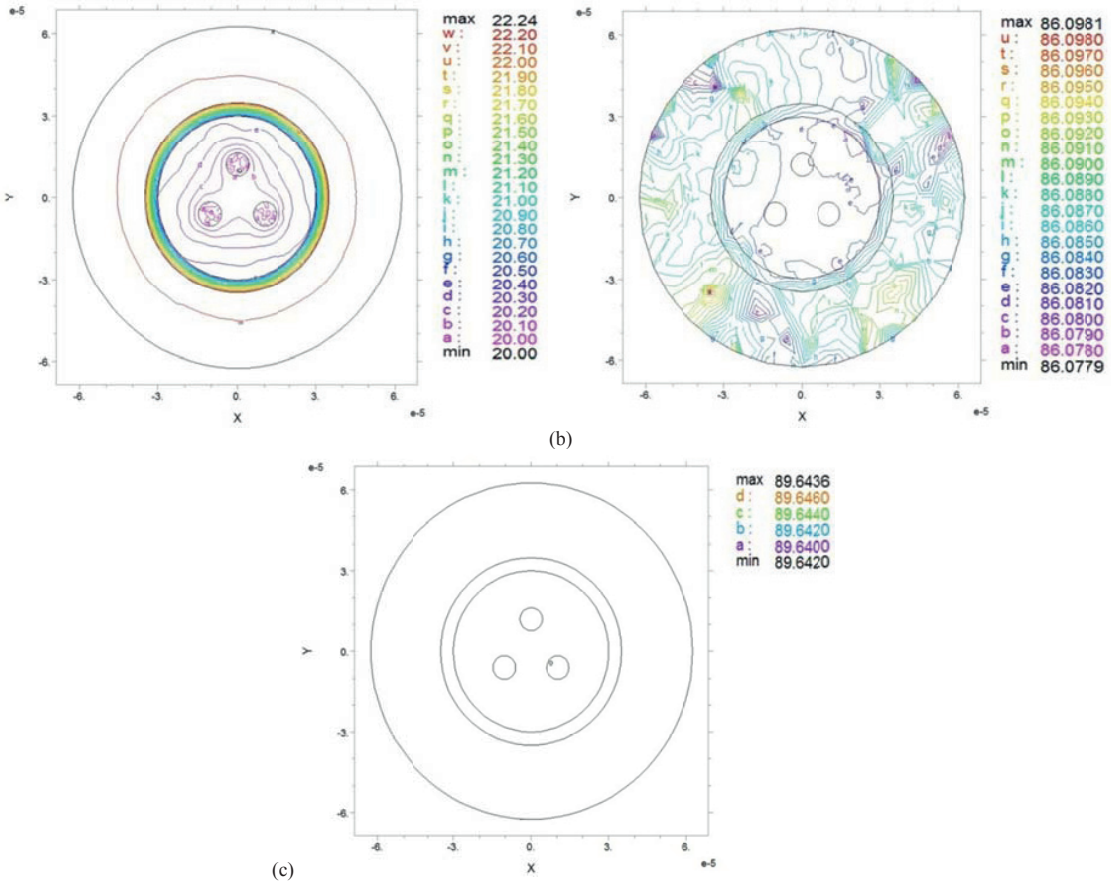

(a) (b)

(c)

Fig. 11. Cross-sectional temperature distribution of the fiber with the triple-circular microchannel for water flow with velocity 0.005 m s^{-1} and temperature 20°C and an external temperature of 90°C: (a) inlet temperature, (b) middle temperature, (c) outlet temperature.

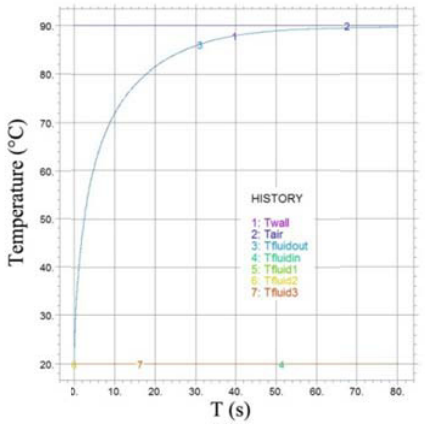

Fig. 12. Temperature with respect to time for water flow (in triple-circular microchannel) with velocity of 0.005 m s^{-1} and initial temperature of 20ºC for an external temperature of 90°C.

4. Discussion

We have presented a study of SiO_2-based microstructure fibers, with cross sections containing circular or elliptical holes, or more complex cross-sectional geometries, as microfluidic devices. The case of the single circular microchannel surrounded by a ring of air can be seen as nothing else than an approximation of an air guiding photonic crystal fiber with a typical fine mesh lattice that forms the band gap structure[13]. The elliptical structures are variations based on the so-called "grapefruit" fiber designs[13]. Based on the possibility of flexible fiber designs (which can be achieved using PMMA as a host material - see future work), the rationale behind this work is to couple the fluid transport to the transfer of heat into the fiber, creating local changes in the behavior of the fluid system.

Therefore, the time-dependent Navier-Stokes equations can be numerically analyzed along with the convection-diffusion equation, in order to ascertain the effects of flow rates, fluid viscosity and the channel diameter. The role of heat flux has been considered in relation to the fluid characteristics. This work is of importance as one cannot assume that the flow dynamics in microstructure fibers will be the same as conventional microfluidics channels. Through the study of the heat transfer, for low Reynolds numbers, we have confirmed anticipated behavior of the fluids in the micro-channel structure. Our approach proves to be versatile for all cases examined; the model can easily be extended for other configurations, such as multiple circular or elliptical microchannels, surrounded (or not) by, a ring of gas (not necessarily air), or instead by a ring consisting of small circles, or complex ellipses. We are extending this work to consider the waveguide properties under different heat and flow regimes.

Further future projects could include comparison with PMMA-based microstructures, validation with experiments, and incorporating electromagnetic effects.

Acknowledgements

The authors acknowledge the co-financing by the Cyprus Research Promotion Foundation and the European Fund of Regional Growth of the EU under the project ΑΝΑΒΑΘΜΙΣΗ/ΠΑΓΙΟ/308/27.

References

1. Kerbage C, Eggleton BJ. Manipulating light by microfluidic motion in microstructured optical fibers. *Opt. Fib. Tech.* 2004;10:133-149.
2. Hassani A, Skorobogatiy M. Design of the microstructured optical fiber-based surface plasmon resonance sensors with enhanced microfluidics. *Opt. Express* 2006;14:11616-11621.

3. Sazio PJA, Amezcua-Correa A, Finlayson CE, Hayes JR et. al. Microstructured optical fibers as high-pressure microfluidic reactors. *Sciencewww.sciencemag.org*, *Science* 2006;311(5767):1583-1586.
4. Yahng JS, Jeoung SC, Choi DS, Cho D, Kim JH, Choi HM, Paik JS (2005). Fabrication of microfluidic devices by using a femtosecond laser micromachining technique and μ-PIV studies on its fluid dynamics. *J. Korean Phys. Soc.* 2005;47(6): 977-981.
5. Colin T, Tancogne S. Stability of bifluid jets in microchannels. *European Journal of Mechanics B/Fluids* 2011;30:409-420.
6. Sahu KC, Valluri P, Splet PDM, Matar OK. Linear instability of pressure-driven channel flow of a Newtonian and a Herschel-Bulkley fluid. *Phys. Fluids* 2007;19:122101.
7. Lien V, Vollmer F. Microfluidc flow rate detection based on intefrated optical fibre cantilever. *Lab Chip* 2007;7:1352-1356.
8. Beskok A, Karniadakis GE. Simulation of heat and momentum transfer in complex microgeometries. *J. Thermophys. Heat Transfer* 1994;8:647-655.
9. Chen K, Wu T-E. Thermal analysis and simulation of a microchannel flow in miniature thermal conductivity detectors. *Sens. Actruators A* 2000;79:211-218.
10. Damean N, Regtien PPL, Elwenspock M. Heat transfer in a MEMS for microfluidics. *Sens. Actruators A* 2003;105:137-149.
11. Plouffe BD, Lewis LH, Murthy SK, Computational design optimization for microfluidic magnetophoresis, *Biomicrofluidics* 2011;5:013413.
12. Kandlikar SG et al. *Heat transfer and fluid flow in minichannels and microchannels*. Elsevier; 2006.
13. Yu R.-j, Zhang B, Chen M-y, Huo L, Tiam Z-g, Bai X-z. A new solution of reducing polymer optical fiber losses. *Optics Communications* 2006;266:536–540.